Latin American Journal of Solids and Structures
www.lajss.org

Dynamic responses and damages of water-filled cylindrical shell subjected to explosion impact laterally

Abstract

An account is given of some principal observations made from a series of experiments in which metal cylindrical shells were subjected to lateral explosion impact by different TNT charge mass and stand-off distance. These cylindrical shells were filled with water in order to identify the main effects produced by the fluid-structure interaction. In comparison, the explosion impact experiments of the empty cylindrical shells were also carried out. The effects of TNT charge mass, stand-off distance, cylindrical shell wall thickness and filled fluid (water) on perforation and deformation of metal cylindrical shells were discussed, which indicated that water increased the wall strength of the cylindrical shells under explosion impact loading, and the buckling deformation and perforation of the cylindrical shell was significantly influenced by the presence of the water; blast-resistant property of the tube under explosive impact loading of 200g TNT charge was much excellent; deformation and damage of empty cylindrical shell were more sensitive to stand-off distance changed. ALE finite element method was employed to simulate the deformations and damages of empty and water-filled cylindrical shells under explosion impact loading. The experimental and computational results are in agreement, showing the validity of the computational scheme in complex fluid-structure interaction problems involving metal materials subjected to explosion impact. The results show that internal pressure of water will increase when subjecting to impact loading, the anti-blast ability of tube structure is significantly enhanced.

Keywords

Mechanics of explosion; Explosion impact; Fluid-structure interaction; water-filled cylindrical shell; Numerical simulation

FuYin Gao [a]
Chong Ji [b]
Yuan Long [c]
KeJian Song [d]

[a] College of Field Engineering, PLA Univ. of Sci. & Tech., China
blastinggaofuyin@163.com
[b] College of Field Engineering, PLA Univ. of Sci. & Tech., China
blasting-captain@163.com
[c] College of Field Engineering, PLA Univ. of Sci. & Tech., China
long_yuan @sohu.com
[d] College of Field Engineering, PLA Univ. of Sci. & Tech., China
song_kejian @163.com

1 INTRODUCTION

Pipeline systems are extensively used in industries such as nuclear, gas and petroleum to transport the flammable or non-flammable liquid or gas. It may be a case that a catastrophic event would occur when these pipelines are subjected to explosion impact loading and damage. Thus, it is necessary to investigate the dynamic response and damage of the thin-walled cylindrical shell, as well as to draw up modified design criteria for such structures. Many studies concerning the deformation, cracking and perforation of thin-walled tubes subjected to lateral impact have been conducted, like W.J.Schuman Jr (1963, 1965), Gefken, P.R *et al.* (1988), Jiang, J. and Olson, M.D (1991,1993), Li, Q.M. and Jones, N. (1995), Chung Kim Yuen *et al.* (2013).

For the pipelines to transport the gas or oil the filled-medium structure interaction are often an important loading, and there have been rather fewer number of studies where deformations and damages of filled-medium cylindrical shell subjected to lateral explosion impact loading have been sought. In fact when the fluid is present, the bulk compression of the fluid and its inertia will produce a back-pressure on the inner walls of pipes. This back-pressure prevents the pipe walls from deforming freely in the work of G.Y. Lu *et al.* (2007). Nishida M. *et al.* (2001) made an experimental investigation on the dynamic behavior of an empty tube and a water-filled tube subjected to spherical projectile impact. It was found that the diameter of the plug of the water-filled tube was slightly larger than that of the plug of the empty tube. But the research of Qasim H. Shah *et al.* (2011) found that deformations of the water-filled pipes were smaller compared with the empty pipes subjected to orthogonal and oblique impacts. Different effects of the filled media on the pipes subjected to impact loads indicate that there appears to be a lack of data on experiments involving fluid-structure interactions in pipeline systems, which might be useful in clarifying the underlying mechanics of the impact event. Currently, impact analyses have been typically done by numerical simulation in some fields, like Dey S. *et al.* (2005), Kurtaran H. *et al.* (2003), Knight Jr NF *et al.* (2000), Motta A.A. (2003), Sanchez-Galvez V. *et al.* (2005). A non-linear finite element code of LS-DYNA was used to follow the experimental results and the ballistic limits of target materials were investigated. The development of a finite element code was described by Prinja Nawal K. (1992) that it was able to predict the pipe deformation when the pipe was filled with water.

In the present paper, the experiments on empty (filled with air) and water-filled cylindrical shells of 2.0mm thickness and 2.75mm thickness subjected to explosion impact by 75g TNT charge and 200g TNT charge with different stand-off distances were carried out, focusing mainly on the effects of the filling medium (water), TNT charge mass, stand-off distance and cylindrical shell wall thickness on deformations and damages of metal cylindrical shells. The objective is to study the deformation and damage of water-filled cylindrical shell, compare the amount of deformation and damage to that of empty cylindrical shell and investigate local anti-damaged capability of the cylindrical shell structure. Subsequently predictions of local damage and deformation caused by the explosion impact loading have been simulated using commercial software LS-DYNA with ALE coupling method which has been able to validate the experimental work reliably.

2 EXPERIMENTAL STUDY

2.1 Experimental setup

A few samples of the water-filled cylindrical shell selected for explosion impact testing are shown in Fig. 1. The cylindrical shells were Q235 metal cylindrical shell of 10cm outer diameter, 2mm and 2.75mm thickness and 1m length. The two ends of the cylindrical shell were welded with caps, one of which was air-proofed and the other was then air-proofed with the unilateral valve after the cylindrical shell was filled with water. It was assured that welding caps were firmly held onto the tube ends and the water did not leak with explosion impact. The filling medium, tap water at atmospheric pressure and room temperature, was carefully poured so that no air bubbles entered the cylindrical shell. In comparison, Fig. 2 shows that the configurations of water-filled and empty cylindrical shell are in the same wall thickness, stand-off distance and TNT charge. The end of the empty cylindrical shell was not close but as open. The reason for this is that the air has good compressibility, and impact events take place in few milliseconds therefore the cylindrical shell ends play little role in deformation process and are not required to create close end. The sketches of the apparatus used for impact experiments are shown in Fig. 3. The cylindrical shells were simply supported on the stent. The contact area between the cylindrical shell and the stent was set to be small so that it would not affect the experimental results. The explosion sources were 75g column TNT charge with dimension $3\times7\text{cm}^2$ and 200g bulk TNT charge with dimension $10\times5\times2.5\text{cm}^3$ respectively. The charge mass was secured above the cylinder and aligned with a line passing through its center. Meanwhile, the model was horizontally suspended with triangular shelves at stand-off distances ranging from 11cm to 4cm. An 8 type electronic detonator is used to initiate the blasting event.

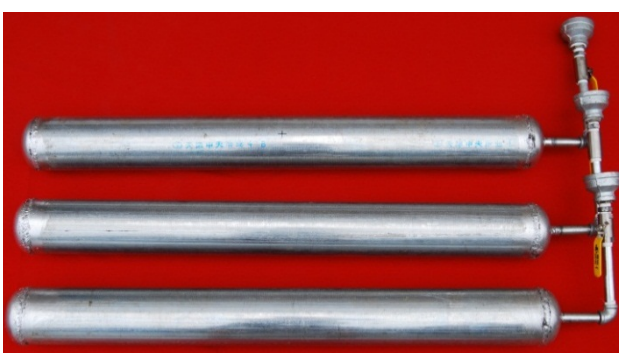

Figure 1: Water-filled cylindrical shell.

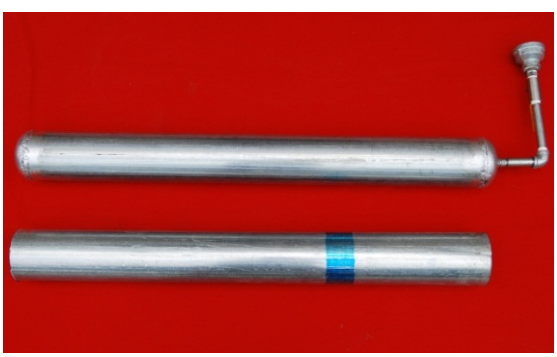

Figure 2: Comparison of water filled and empty cylindrical shell.

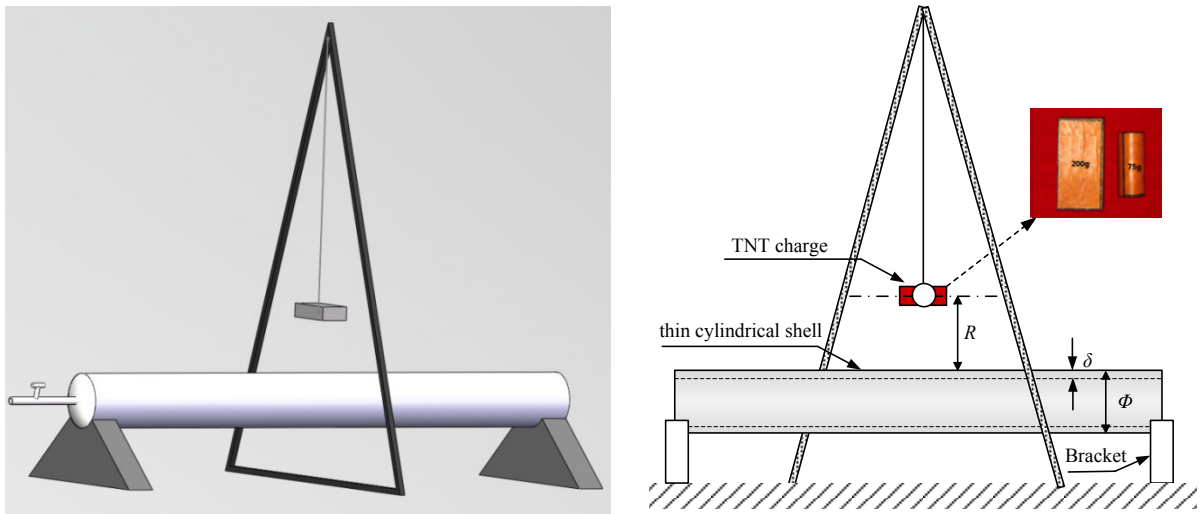

Figure 3: Sketches of experiment setup.

2.2 Experimental results

(a) 75g TNT charge and 2.0mm thickness.

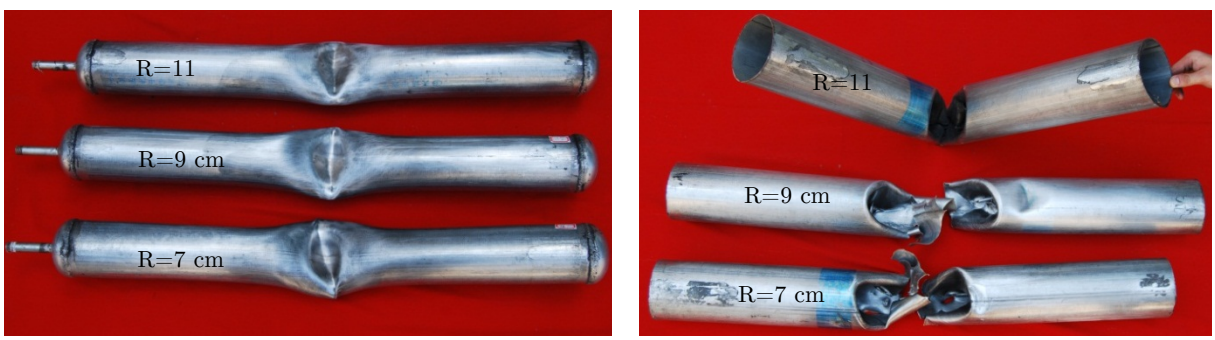

(b) 200g TNT charge and 2.0mm thickness.

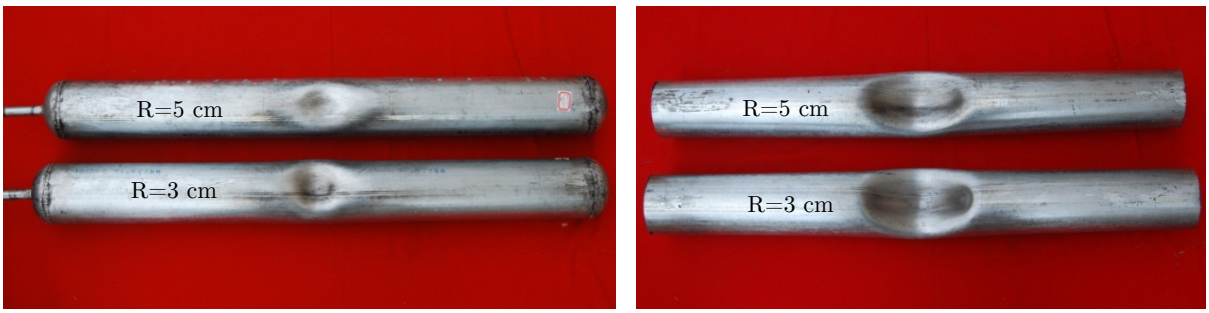

(c) 75g TNT charge and 2.75mm thickness.

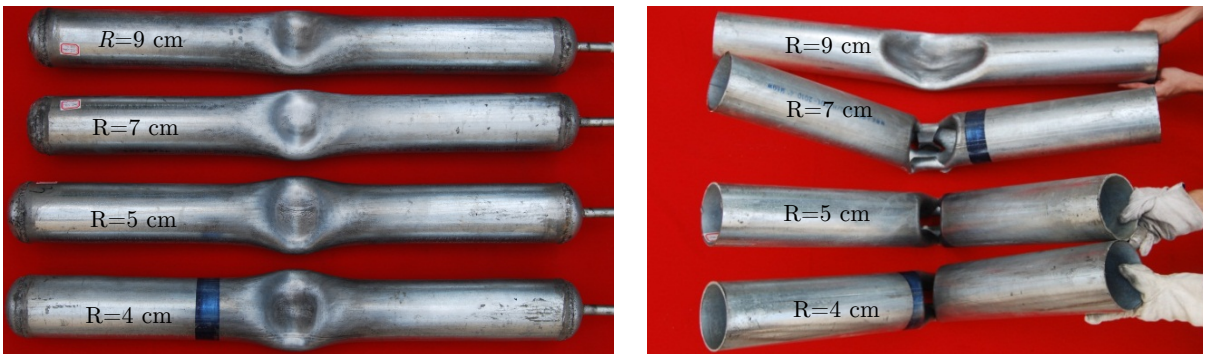

(d) 200g TNT charge and 2.75mm thickness.

Figure 4: Sunken deformations and damages of the water-filled (left) and empty (right) cylindrical shell.

Fig.4 gives sunken deformations and damages of the cylindrical shell after lateral explosion impact (The cylindrical shells with vessel are filled-water pipe, the others are empty pipe). From Fig.4 it is shown that local sunken deformations were generated on the cylindrical shell under lateral explosion impact loading, sunken nests were observed; the cylindrical shell wall near the point of impact was deformed and even perforated, which expanded in both axial and circumferential directions and was especially distinct for the thin cylindrical shell. With the presence of the water the deformation and damage became small, which may indicate that the fluid localizes the impact deformation of the cylindrical shell wall and increase the strength of the cylindrical wall.

Therefore, the attention is focused on the observation of both the deformation and damages of the cylindrical shell wall in the vicinity of the impact point. The plastic deformation of the water-filled cylindrical shell under explosion impact of 75g TNT charge was more localized near the impact point and was smaller than that of the empty cylindrical shell of the same condition in both axial and circumferential directions; the deformation sketch is like an ellipse when looking down from the impact direction, the ratio of which between the long axis and the short axis is in the range of 0.8 to 1.3. In comparison with 75g TNT charge the deformation extents and shapes of the cylindrical shell under explosion impact of 200g TNT charge are larger. Meanwhile, a large overall structural deflection of the cylindrical shell occurs, but perforation failure is not generated. Damaged manner of wall-filled cylindrical shell after 200g TNT explosion impact loading is bending deformation of forming sunken nest, but that of empty cylindrical shell is mainly perforation failure. In conclusion, for given TNT charge mass, stand-off distance and wall thickness the damaged extent

of water-filled cylindrical shell is smaller than empty cylindrical shell, which indicates that the blast-resistant property of the water-filled cylindrical shell under explosion impact loading is stronger than that of the empty cylindrical shell in the same condition. This feature is different from that the water can decrease the ballistic limit of the tube wall under impact of the projectile, like S.Y. Zhang *et al.* (2007), Nishida M. *et al.* (2001, 2006).

2.3 Discussion

Experimental results have indicated that the empty and water-filled cylindrical shell were subjected to lateral explosion loading to assess the difference in deformation and damage modes of the cylindrical shell. Although the deformations of the water-filled cylindrical shell is smaller than that of the empty cylindrical shell subjected to explosion impacts and the stresses generated in the water filled pipes are higher, the support provided by the water reduces the maximum deflection and consequently improves the level of tensile strain induced by the membrane action and the water filled cylindrical shell is little vulnerable to damage and failure. There are many reasons for this problem, and some of the most significant ones will be briefly discussed in the following.

2.3.1 Influence of charge mass on dynamic response of cylindrical shell

Undoubtedly, the peak value of the pressure with 200g TNT charge mass at the face midpoint of the cylindrical shell is higher than that of 75g TNT charge mass in the same condition, which is the reason that the deformation and damage extent of the cylindrical shell subjected to explosion impact of 200g TNT charge is more severe than that of 75g TNT charge. Although deformation extent of the empty and water-filled cylindrical shells subjected to explosive impact of 75g TNT charge is different, the plastic deformation modes of forming local sunken nest are identical and perforation failure mode does not appear among the most cylindrical shells. The deformation and damage modes of water-filled cylindrical shells subjected to explosive impact of 200g TNT charge are also the plastic deformation, but that of most empty cylindrical shells are perforation failure. In other words, blast-resistant property of the water-filled cylindrical shell under explosive impact loading of 200g TNT charge is more excellent.

2.3.2 Influence of stand-off distance on dynamic response of cylindrical shell

From Fig. 5, it can be seen that the axial deformation curve of the cylindrical shell with 2.0mm thickness subjected to explosive impact of charge mass and the stand-off distance. The behavior concurs with previous work on free field explosions, as blast peak overpressure decreases with increasing stand-off distance, like Kinney K. F. (1962), Baker W. E. (1973), Smith P. D. and Hetherington J. G. (1994), Wharton R. K. *et al.* (2000). Not surprisingly, the flat curve is observed with an increase in stand-off distance, the changed trend of which is identical to that of 2.75mm cylindrical shell. For water-filled cylindrical shell, there is the same deformation mode in stand-off distances ranging from 11 to 3 cm, only deformation extent of which is gradually larger with decreasing stand-off distance. From Fig. 4 it is shown that the deformation and damage mode of empty cylindrical shell subjected to explosive impact is changed with decreasing stand-off distance, which indicates dynamic responses of empty cylindrical shell subjected to explosion impact loading are sensitive to stand-off distance changed.

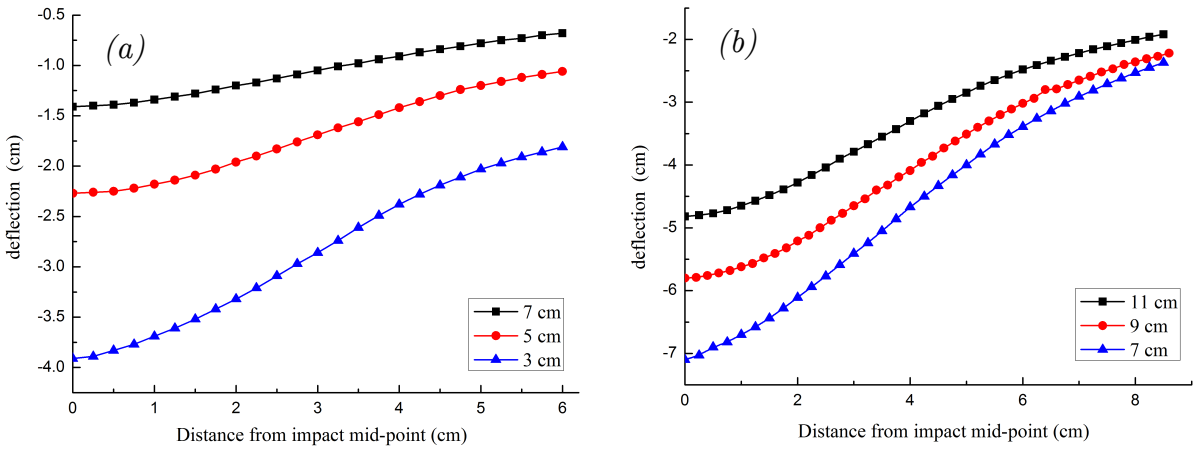

Figure 5: Axial deformation curve on cross-section of the water-filled cylindrical shell with 2.0mm thickness: (a) 75gTNT charge (b) 200gTNT charge.

2.3.3 Influence of thickness on dynamic response of cylindrical shell

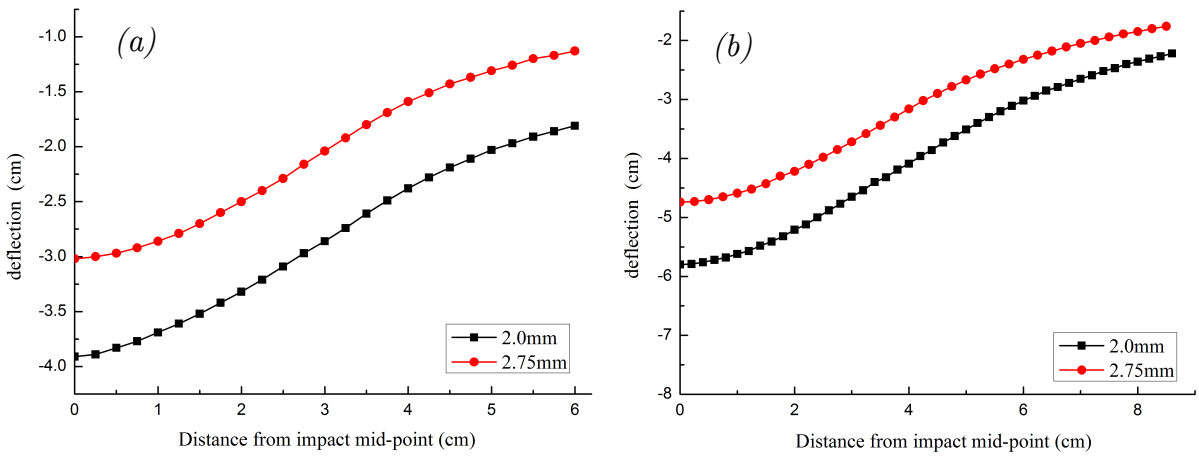

Figure 6: Axial deformation curve on cross-section of the water-filled cylindrical shell: (a) 75gTNT charge and stand-off distance 3cm (b) 200gTNT charge and stand-off distance 9cm.

The empty cylindrical shell wall strength increases with increasing thickness of the cylindrical shell wall. It is noticeable that the deformation and damage extent of 2.0mm thickness is larger in comparison with 2.75mm thickness cylindrical shell for given charge mass and stand-off, and even 2.0mm thickness cylindrical shell wall in many tests is penetrated while 2.75mm thickness cylindrical shell is only deformed. With the presence of water the energy acted on the water-filled cylindrical shell is absorbed by water and the cylindrical shell, so the blast-resistant ability of water-filled cylindrical shell is different from that of empty cylindrical shell. By comparing the sunken nest shape with explosive impact it can be noticed that the sunken nest of the cylindrical shell of 2.0mm thickness after explosive impact is bigger than that of 2.75mm thickness, which is more obvious in the circumferential direction. Fig. 6 shows that the axial deformation curve of water-filled cylindri-

cal shells with explosive impact, and it can be seen that the axial cylindrical shell deformation between 2.0mm thickness and 2.75mm thickness shows some difference but overall deformation trend is yet in good agreement with plastic deformation. In practical engineering, thick cylindrical shell wall is selected for improving blast-resistant feature of empty cylindrical shell. Instead, for water-filled cylindrical shell, it is most important to select appropriate wall thickness of cylindrical shell. The thick wall of cylindrical shell which is not economic and efficient is normally not applicable for transporting gas and petroleum, as well as thin wall of cylindrical shell due to its poor wall strength which is potentially dangerous.

3 ARBITRARY-LAGRANGIAN-EULERIAN (ALE) FINITE ELEMENT METHOD

Due to the high deformability of the cylindrical shell, a strong fluid-structure interaction takes place during the shock wave loading and carefully designed coupled fluid-solid solver is necessary to capture the response of the cylindrical shell. The ALE method is based on the arbitrary movement of a reference domain, which will correspond to the finite element mesh. As detailed in the work of T.J.R. Hughes *et al.* (1981), this domain is introduced as a third domain additionally to the common material and spatial domains. These domains correspond to the Lagrangian and Eulerian domains, respectively. In ALE solver, the air-blast problem is formulated in the coordinate of the reference domain. By combining the ALE solver with an Eulerian-Lagrangian coupling algorithm, a structural or Lagrangian mesh can interact with the gas products or Eulerian mesh. This technique was used for the ranges where the simplified blast model produced uncertain impulse duration as a result of blast proximity.

The total time derivative of a variable f with respect to a reference coordinate can be described as:

$$\frac{df(\vec{X},t)}{dt} = \frac{\partial f(\vec{x},t)}{\partial t} + (\vec{v} - \vec{w}) \cdot \overrightarrow{grad} f(\vec{x},t) \tag{1}$$

where $\vec{X}$ is the Lagrangian coordinate, $\vec{x}$ is the ALE coordinate, $\vec{v}$ is the particle velocity and $\vec{w}$ is the velocity of the reference coordinate, which will represent the grid velocity for the numerical simulation, and the system of reference will be later the ALE grid. Thus substituting the relationship between the total time derivative and the reference configuration time derivative derives the ALE equations.

Let $\Omega^f \in R^3$ represents the domain occupied by the fluid particles, and let $\partial\Omega^f$ denotes its boundary. The equations of mass, momentum and energy conservation for a Newtonian fluid in ALE formulation in the reference domain are given by

$$\frac{\partial \rho}{\partial t} + \rho div(\vec{v}) + (\vec{v} - \vec{w}) grad(\rho) = 0 \tag{2}$$

$$\rho \frac{\partial \vec{v}}{\partial t} + \rho(\vec{v} - \vec{w}) \cdot \overline{\overline{grad}}(\vec{v}) = \overrightarrow{div}(\overline{\sigma}) + \vec{f} \tag{3}$$

$$\rho \frac{\partial e}{\partial t} + \rho(\vec{v} - \vec{w}) \cdot \overrightarrow{grad}(\vec{e}) = \overline{\sigma} : \overline{\overline{grad}}(\vec{v}) \tag{4}$$

where ρ is the density and σ is the total Cauchy stress given by

$$\overline{\overline{\sigma}} = -p \cdot \overline{\overline{Id}} + \mu(\overline{\overline{grad}}(\vec{v}) + \overline{\overline{grad}}(\vec{v})^T) \tag{5}$$

where p is the pressure and μ is the dynamic viscosity.

For compressible flow, Eqs.(2)-(4) are completed by an equation of state that relies pressure to density and internal energy. In the energy Eq. (4), e is the internal energy by unit volume, the temperature is computed using an average heat capacity C_v:

$$\rho e = C_v \cdot T \tag{6}$$

Eqs.(2)-(4) are completed with appropriate boundary conditions.

The approach for solving ALE formulation of Navier-Stokes Eqs.(2)-(4) is referred to as an operator split in the literature of C.J. Freitas *et al.* (1996) and B. Van Leer *et al.* (1977) where the calculation for each time step is divided into two phases. The ALE method begins working as a Lagrangian finite element code in which the motions of the fluid and the structure are determined and the finite element grid is deformed following the material. As long as the mesh distortion is acceptable, the Lagrangian calculation continues. If it becomes highly distorted, the second step (the advection step) is performed. In the ALE methodology the distorted mesh can be partially restored to its original shape based on predefined criteria for element deformation. Following a prescribed measure of permissible distortion in the element, the element shape is changed; and mass, momentum and energy are fluxed across the old element boundaries to calculate their new values for the new element shape. In general, the ALE methodology permits flow of material across element boundaries preserving a balance for the physical velocity between grid motion and flow. The second-order Van Leer advection algorithm is employed in the numerical applications to ensure a higher accuracy.

4 NUMERICAL SIMULATIONS

The numerical simulations of a partially water-filled cylindrical shell subjected to explosion impact loading are performed with the commercial finite element code LS-DYNA applying the Arbitrary Lagrangian Eulerian (ALE) technique for the fluid.

4.1 Finite element model

The ALE model of the cylindrical shell involves five different material types. The first material model represents metallic cylindrical shell, followed by the TNT cylindrical explosion charge, the filled water, the stent and finally the surrounding air media, which is used to fill the space affected by the explosion charge. Note that in the purely Lagrangian approach, only one type of material model is needed, namely for the metallic cylindrical shell. The stent is rigid body. The contact between the stent and the cylindrical shell has been defined as Contact Automatic Surface to Surface. The mesh size of the air, water, TNT charge and stent is 0.25cm. The refined mesh of 0.125 cm for the tube from midpoint to 10 cm away from midpoint was used, the other part of which is mesh of 0.5cm. By using the inherent symmetry of the studied problem, calculation time can be saved. Thus, only a quarter of the cylindrical shell was modeled with the appropriate boundary conditions ap-

plied along the symmetry planes. Fig.7 shows the model of 200g TNT explosion impact loading constructed with SOLID164 solid element and g-cm-μs unit.

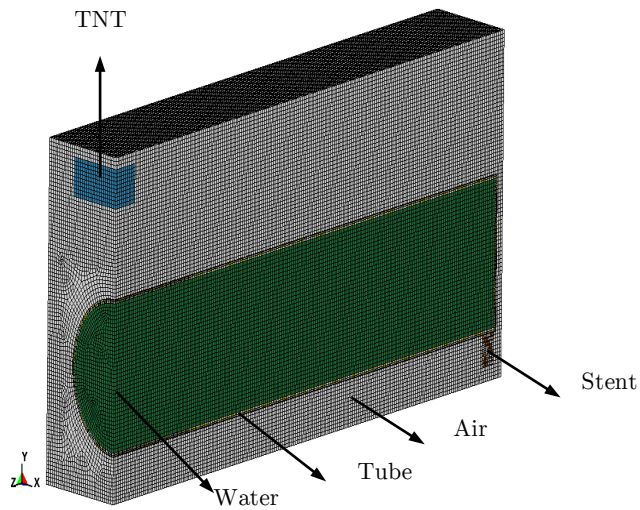

Figure 7: The finite element model.

4.2 Material behavior

The Jones-Wilkens-Lee (JWL) equation of state (EOS) models the pressure generated by the expansion of the detonation product of the chemical explosion. It has been widely used in engineering calculations in the Livermore Software Technology Corporation (LSTC) (2003) and can be written as

$$P = A_1\left(1-\frac{\omega}{R_1V}\right)e^{-R_1V} + B_1\left(1-\frac{\omega}{R_2V}\right)e^{-R_2V} + \omega\frac{E}{V} \tag{7}$$

where A_1, R_1, B_1, R_2 and ω are material constants, P is the pressure, V is the relative volume of detonation product and E is the specific energy with an initial value of E_0. The TNT explosions C-J parameters and the JWL equation of state parameter: ρ_e =1.61g/cm^3, D =6.93km/s, p_{CJ} =21.0GPa, A_1=371.2GPa, B_1=3.231GPa; R_1=4.15, R_2=0.95; ω=0.30; E_0=7.0×109J/m^3, respectively.

Material Type 9 of LS-DYNA (*MAT_NULL) is used to calculate the pressure P from a specified EOS, which defines the relationship between pressure, density and internal energy. As for the air, the polynomial EOS is usually employed, in which the pressure P is expressed as

$$P = C_0 + C_1\mu + C_2\mu^2 + C_3\mu^3 + (C_4 + C_5\mu + C_6\mu^2)e \tag{8}$$

where e is the internal energy per volume. The compression of the material is defined by the parameter $\mu = \rho/\rho_0 - 1$ with ρ and ρ_0 being the current and initial density of the material, respectively. As a matter of fact, the air is often modeled as an ideal gas by setting

$C_0 = C_1 = C_2 = C_3 = C_6 = 0$ and $C_4 = C_5$=0.401. Air mass density ρ_0 and initial internal energy e_0 are 1.29 kg/m^3 and 0.25 J/cm^3, respectively.

To model water, the combination of Grüneisen EOS associated with the *MAT_NULL is adopted. The values of coefficients used to characterize the EOS of the water are typical in this kind of problem. Water mass density ρ_0=1000.0 kg/m^3 and Grüneisen parameter γ_0 = 0.50.

The Johnson-Cook (J-C) model in the work of Johnson GR and Cook WH (1983) is used to study the dynamic mechanical behavior of the cylindrical shell, which has been frequently used in impact analysis due to its simplicity. The equivalent stress is expressed as

$$\sigma_y = \left[A + B\left(\bar{\varepsilon}^p\right)^n\right]\left[1 + C\ln\dot{\varepsilon}^*\right]\left[1 - \left(T^*\right)^m\right] \tag{9}$$

where A, B, C, n and m are the J-C material coefficients, ε^p is the effective plastic strain, $\dot{\varepsilon}^* = \dot{\bar{\varepsilon}}^p / \dot{\varepsilon}_0$ is the effective plastic strain rate at a reference strain rate $\dot{\varepsilon}_0 = 1s^{-1}$, and the homologous temperature T^* is defined by $T^* = (T - T_r)/(T_m - T_r)$, where the suffixes r and m indicate room and melting temperatures, respectively. The Johnson-Cook fracture criterion is expressed as

$$\varepsilon_f = [D_1 + D_2 \exp D_3\sigma^*][1 + D_4 \ln\dot{\varepsilon}^*][1 + D_5 T^*] \tag{10}$$

where $D_1, \ldots, D_5$ are material constants. σ^* is the stress triaxiality ratio. The damage D of a material element is expressed as $D = \sum \Delta\varepsilon / \varepsilon_f$, $\Delta\varepsilon$ is the increment of accumulated (equivalent) plastic strain that occurs during an integration cycle and ε_f is the fracture strain. Material parameters of the metallic cylindrical shell in the work of XIAO Xin-ke (2010): ρ=7.8g/cm^3, A=229.0 MPa, B=439.0, MPa, n=0.503, C=0.1, m=0.55, D_1=0.3, D_2=0.9, D_3=-2.8, D_4=0.0, D_5=0.0.

4.3 Validation of the numerical approach

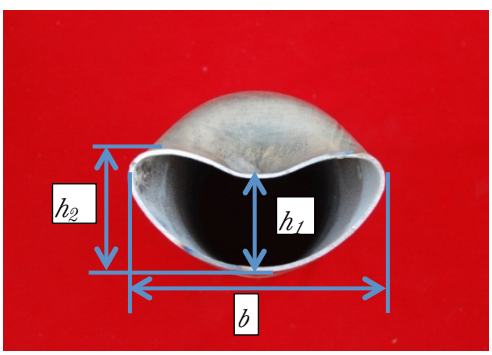

(a) A sample tube section after explosion impact

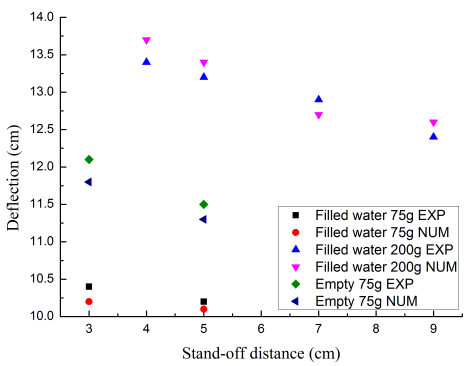

(b) b

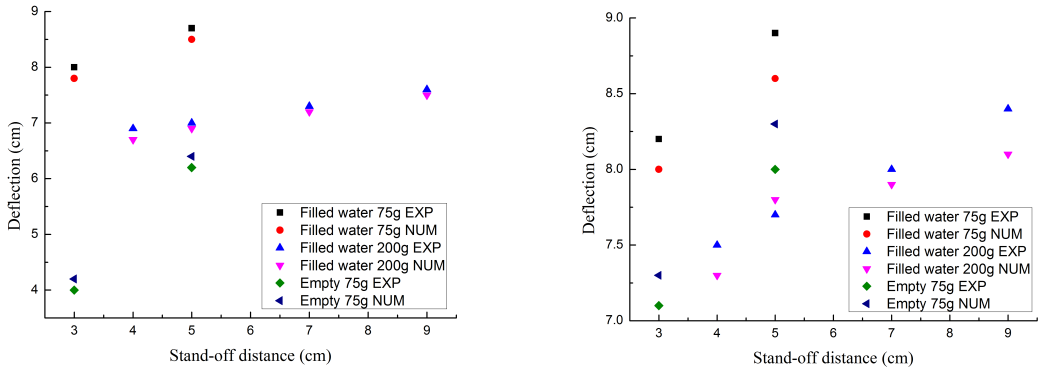

Figure 8: Comparison between experimental and numerical results dent size along the cross section of the cylindrical shell.

The comparison with experimental data for situations of the same explosion impact loading is essential for demonstrating the validity of the numerical method adopted. Since plastic deformation and damage of the cylindrical shell near the impact point is larger in comparison with the overall cylindrical shell, the sunken nest generated by explosion impact loading can embody the extent of deformation and damage of the cylindrical shell. As shown in Figs. 8 (a), the dent size was measured along the cross section of the cylindrical shell where the diameter of the cylindrical shell has increased and it was defined as dent size. Detailed experimental results are shown in Figs. 8 where the effects of the pipes on their deformation pertaining to dent width and diameter change is compared to the results obtained from numerical simulation. From Fig 8, it can be seen that the simulation results in all the cases are in agreement with the experimental results though some very small discrepancies are evident. The discrepancies can be overcome with further investigations. Because the typical values along the cross section of the cylindrical shell with penetration damage can be accurately measured.

As already stated, the agreement between the numerical and experimental results shown in Fig. 9 is, taking the complexity of the simulated problem into account, excellent. This clearly indicates that numerical simulations of the present deformation and perforation problem using properly ALE coupling models are able to describe the main physical mechanisms and provide reliable results. Thus, it seems relatively adequate to use this model in a forthcoming optimization study of the cylindrical shell subjected to the explosion impact loading.

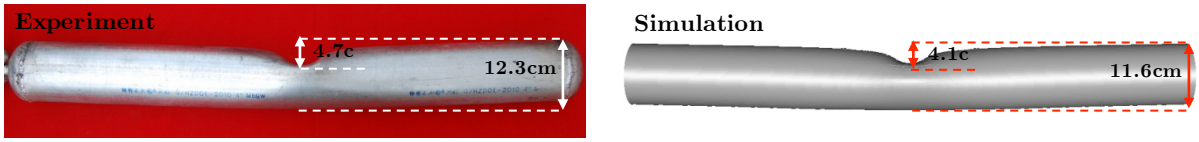

(a) 2.75mm water-filled cylindrical shell, stand-off distance 9cm and 200g TNT charge

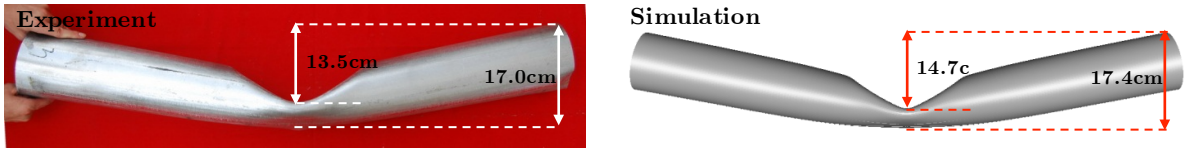

(b) 2.75mm empty cylindrical shell, stand-off distance 9cm and 200g TNT charge mass.

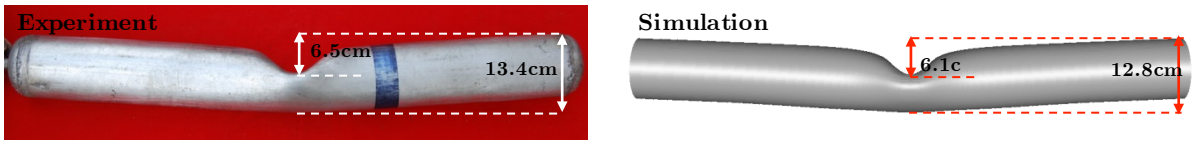

(c) 2.75mm water-filled cylindrical shell, stand-off distance 4cm and 200g TNT

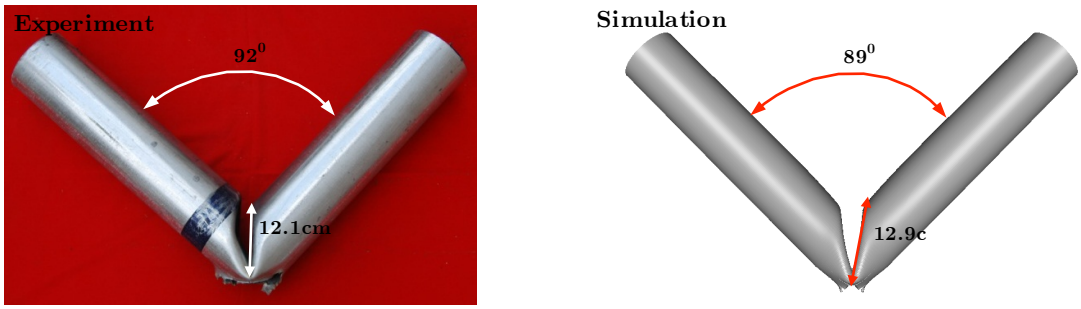

(d) 2.75mm empty cylindrical shell, stand-off distance 4cm and 200g TNT charge

Figure 9: The comparison of experiment and simulation of the deformation of cylindrical

4.3 Numerical analysis

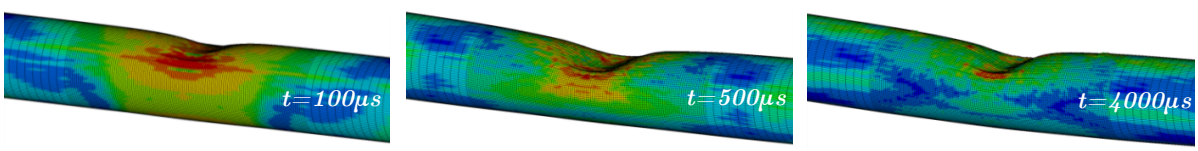

(a) 2.75mm water-filled cylindrical shell, stand-off distance 9cm and 200g TNT charge mass

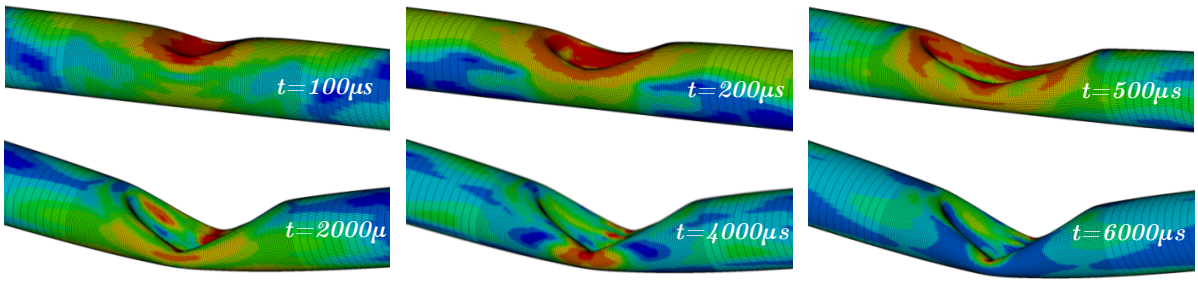

(b) 2.75mm empty cylindrical shell, stand-off distance 9cm and 200g TNT charge mass

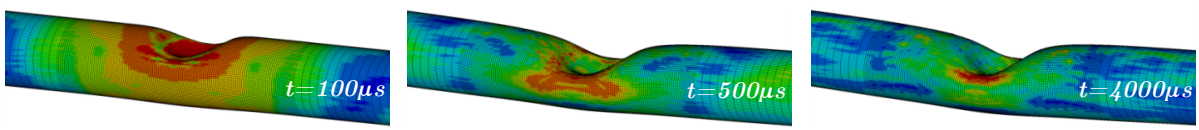

(c) 2.75mm water-filled cylindrical shell, stand-off distance 4cm and 200g TNT

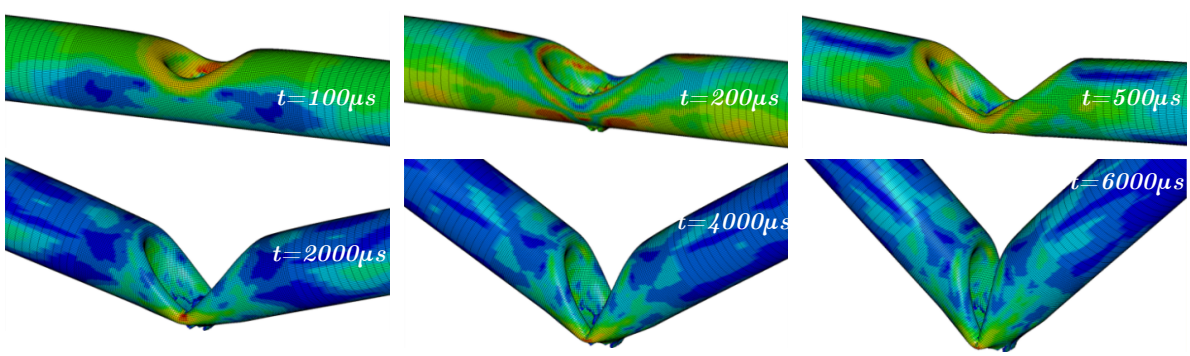

(d) 2.75mm empty cylindrical shell, stand-off distance 4cm and 200g TNT charge

Figure 10: Deformation processes of the cylindrical shells.

Deformation process of metal cylindrical shells is shown in Fig. 10. It can be see that local axial size of sunken zone is the biggest at 500μs in Fig. 10 (a), and then the back side slowly bent, the deformation of the cylindrical shell is not developed at 4000μs; final axial size of local sunken zone is slightly decreased. In Fig. 10 (b), the section in center of cylindrical shell is seriously flat, bending strength of which is weaken in a certain degree. In comparison with Fig. 10 (a), the face and back of the tube in Fig. 10 (b) are more bent, but local sunken deformation accounts for a dominant position. For Fig. 10 (c), the deformation of the tube section is much flatter than Fig. 10 (a). When explosion impact energy acted on the cylindrical shell is not completely dissipated by local sunken deformation, the whole cylindrical shell begins to absorb the energy, overall bending deformation is generated, and the deformation of the tube becomes stable at 4000μs. After the maximum displacement peak, the elastic rebound of the cylindrical shell occurs, resulting in a vibrating response.

In Fig. 10 (d), the radial crack of the face tube is generated by explosion impact loading, after further expansion of the crack; perforation failure takes place on the tube wall. Rupture size increases in axis direction of the tube, then decreases with V-shaped overall deformation. The tube structure is not changed after 6000μs.

The simulation results show that when the TNT charge is detonated, an initial shock wave generates from the center of the charge and propagates outwards rapidly, and the detonation products are produced. When the detonation products propagate downwards to the surface of the cylindrical shell and form overpressure, the deformation appears on the cylindrical shell wall and a force is exerted on the water column inside; then the load is transmitted from the water to the cylindrical shell and back from the cylindrical shell to the water due to the plastic deformation. When the water is present, the deformation is more localized and the bending deformation propagates away from the point of impact at a significantly slower rate.

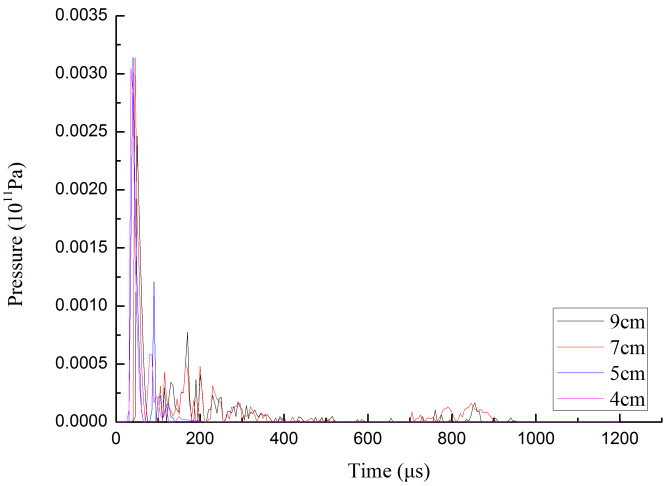

Figure 11: Water pressure-time curves of midpoint of the 2.75mm water-filled cylindrical shell.

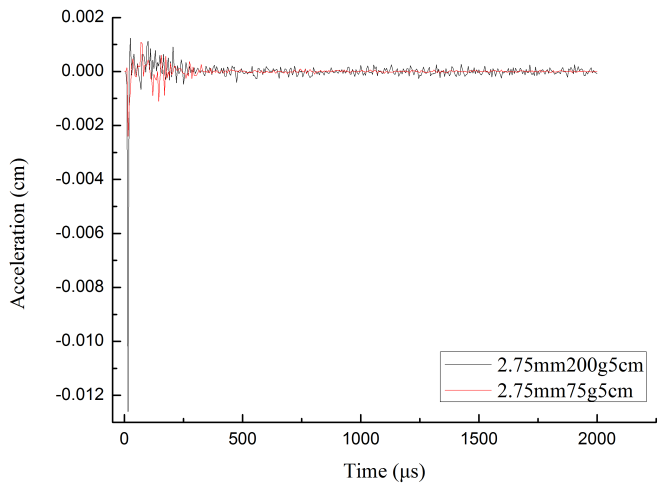

Figure 12: The vertical acceleration-time curve of the water-filled cylindrical shell in impact point.

5 CONCLUSIONS

The deformation and perforation of empty and water-filled metal cylindrical shell subjected to explosive impact by 75g TNT charge and 200g TNT charge with different stand-off distances were investigated. The water filling in the cylindrical shell provides a 'foundation' pressure to resist the deformation, which may affect the deformation process, increase tube wall strength and anti-blast ability of the tube under explosive impact loading. The deformation of the water-filled cylindrical shell was more localized near the impact point and was smaller than that of the empty cylindrical shell.

The experimental results indicated that the deformation and perforation failure of the cylindrical shell wall were significantly influenced by the charge mass, stand-off and wall thickness. Compared with 75g TNT charge the blast-resistant property of the water-filled cylindrical shell subjected to explosive impact loading of 200g TNT charge was more excellent, and the deformation and damage of empty cylindrical shell was more sensitive to stand-off distance changed. For meeting blast-resistant demand, it was important for water-filled cylindrical shell to select appropriate wall thickness.

Excellent agreement between numerical and experimental results shows that the structural response of the cylindrical shell can be efficiently modeled, and the ALE coupling model was able to capture the main trend of deformation and perforation failure in the experiments in an adequate manner.

The high water pressure was generated for resisting deformation of the tube subjected to explosion impact loading, a part of the impact energy is dissipated; the anti-blast ability of tube structure is significantly enhanced.

Acknowledgment

This research was supported by the National Nature Science Foundation of China, No. 11102233 and 51178460.

References

Baker WE (1973), Explosions in air. Austin: University of Texas.

B. Van Leer 1977, Towards the ultimate conservative difference scheme. IV. A new approach to numerical convection, J. Comput. Phys. 23:276–299.

Chung Kim Yuen, S. Nurick, G.N. Brinckmann, H.B., and Blakemore, D (2013)., Response of cylindrical shells to lateral blast load, International Journal of Protective Structures, 4: 209–230.

C.J. Freitas, C.E. Anderson Jr., J.D. Walker, D.L. Littlefield (1996), Hydrodynamic ram: A benchmark suite, in: Structures Under Extreme Loading Conditions, PVPvol. 325, ASME, New York, pp. 63–74.

Dey S, Bo¨ rvik T, Hopperstad OS, Langseth M (2005)., On the influence of constitutive relation in projectile impact of steel plates. Int J Impact Eng; 32:35.

Gefken, P.R., Kirkpatrick, S.W., and Holmes, B.S (1988)., Response of impulsively loaded cylindrical shells, Int J Impact Eng; 7: 213–227.

Jiang, J. and Olson, M.D (1991)., Nonlinear dynamic analysis of blast loaded cylindrical shell structures, Computers & Structures, 41: 41–52.

Jiang, J. and Olson, M.D (1993)., New design-analysis techniques for blast loaded stiffened box and cylindrical shell structures, Int J Impact Eng, 13: 189–202.

Johnson GR, Cook WH (1983). A constitutive model and data for metals subjected to large strain, high strain rates and high temperature. In: Proceedings of the 7th International Symposium on Ballistics, The Hague, The Netherlands, p. 541–548.

Kinney KF (1962). Explosive shocks in air. Macmillan.

Knight Jr NF, Jaunky H, Lawson RE, Ambur DR (2000). Penetration simulation for uncontained engine debris impact on fuselage-like panels using LS-DYNA. Finite Elem Anal Des,36:99.

Kurtaran H, Buyuk M, Eskandarian A (2003). Ballistic impact simulation of a GT model vehicle door using a finite element method. Theor Appl Fract Mech; 40:113.

Li, Q.M. and Jones, N (1995)., Blast loading of a "short" cylindrical shell with transverse shear effects, Int J Impact Eng, 16: 331–353.

Livermore Software Technology Corporation (LSTC) (2003). LS-DYNA keyword user's manual, Version 960. Livermore, CA.

Masahiro Nishida, Koichi Tanaka (2006). Experimental study of perforation and cracking of water-filled aluminum tubes impacted by steel spheres. International Journal of Impact Engineering 32: 2000-2016

Motta AA (2003). Computational ballistics. WIT Press.

Nishida M, Tanaka K, Ito M (2001). Deformation and perforation of water-filled and empty aluminum tubes by a spherical steel projectile: experimental study. Impact engineering and application. p. 375–380.

Prinja Nawal K (1992). Combined beam element for large dynamic motion of whipping pipes with fluid structure inter-action. Finite Element in Analysis and Design, 11:117-152.

Qasim H. Shah (2011). Experimental and numerical study on the orthogonal and oblique impact on water filled pipes. International Journal of Impact Engineering; 38: 330–338.

Sanchez-Galvez V, Brebbia CA, Motta AA, Anderson CE (2005)., Computational ballistics II. WIT Press.

Smith PD, Hetherington JG (1994). Blast and ballistic loading of structures. Butterworth and Heinemann.

S.Y. Zhang, J.P. Lei, J.L. Yang (2007). Dynamic responses and damages of water-filled pre-pressurized metal tube impacted by mass, International Journal of Impact Engineering; 34: 1594–1601.

T.J.R. Hughes, W.K. Liu, T.K. Zimmerman (1981). Lagrangian Eulerian finite element formulation for viscous flows, J. Comput. Meth. Appl. Mech. Eng. 21:329–349.

Wharton RK, Formby SA, Merrifield R (2000)., Air-blast TNT equivalence for a range of commercial blasting explosives. Journal of Hazardous Materials; A79:31–9.

W.J.Schuman Jr (1963)., The response of cylindrical shells to external blast loadings, Aberdeen Proving Ground, Maryland, U. S. Army Ballistic Research Laboratories. 1461: 1–170.

W.J.Schuman Jr (1965)., A failure criterion for blast loaded cylindrical shells, Aberdeen Proving Ground, Maryland, U. S. Army Ballistic Research Laboratories. 1292: 1–128.

XIAO Xin-ke (2010)., The ballistic resistance of double-layer metallic target and the deformation and fracture of Taylor rod[D]. Harbin: Harbin Institute of Technology (in Chinese).